

(CH₂Cl₂): $\bar{\nu}(\text{CO}) = 2004$ (vs), 1947 (sh), 1931 cm⁻¹ (vs). **3**: MS (FAB⁺, CH₂Cl₂): m/z (%): 968 (100) [M^+], 791 (92) [$M^+ - \text{Cp}^{\text{II}}$]; IR (CH₂Cl₂): $\bar{\nu}(\text{CO}) = 2023$ (vs), 1954 cm⁻¹ (vs); ¹H NMR (300 MHz, CDCl₃, 25 °C): rotamer **3a**: $\delta = 7.18$ (d, $J(\text{H,H}) = 2.4$ Hz, 2H, H4 and H5), 6.60 (t, $J(\text{H,H}) = 2.4$ Hz, 1H, H2), 5.94 (d, $J(\text{H,H}) = 2.4$ Hz, 2H, H4 and H5), 5.83 (t, $J(\text{H,H}) = 2.4$ Hz, 1H, H2, Cp^{II}), 4.42 and 4.19 (m, 2H each, =CH, cod), 2.7–2.4 (m, 2H), 1.9–2.2 (m, 4H), 1.8–1.6 (m, 2H, CH₂, cod), 1.32 and 1.26 (s, 18H each, Cp^{II}); rotamer **3b**: $\delta = 6.69$ and 6.38 (t, $J(\text{H,H}) = 2.4$ Hz, 1H each, H2), 6.03 and 5.90 (d, $J(\text{H,H}) = 2.4$ Hz, 2H each, H4 and H5, Cp^{II}), 4.42 and 4.19 (m, 2H each, =CH, cod), 2.7–2.4 (m, 2H), 2.2–1.9 (m, 4H), 1.8–1.6 (m, 2H, CH₂, cod), 1.31 and 1.30 (s, 18H each, Cp^{II}); ¹³C{¹H} NMR (75 MHz, CDCl₃, 25 °C): rotamer **3a**: $\delta = 177.7$ (CO), 150.0 and 142.2 (C1 and C3), 127.6 (C2), 119.7 (C4 and C5), 110.0 (C2), 105.5 (C4 and C5, Cp^{II}), 84.0 and 80.6 (d, $J(\text{Rh-C}) = 11.5$ Hz, =CH, cod), 34.8 and 34.0 (CMe₃), 32.7 and 31.8 (CH₃, Cp^{II}), 31.7 and 30.6 (CH₂, cod); rotamer **3b**: $\delta = 178.3$ (CO), 147.2 and 147.1 (C1 and C3), 123.8 and 120.7 (C2), 109.5 and 108.8 (C4 and C5, Cp^{II}), 85.9 and 80.6 (d, $J(\text{Rh-C}) = 11.5$ Hz, =CH, cod), 34.5 and 34.4 (CMe₃), 32.3 and 32.2 (CH₃, Cp^{II}), 31.6 and 30.2 (CH₂, cod). **4**: ¹H NMR (300 MHz, CDCl₃, 25 °C): $\delta = 6.72$ and 6.62 (t, $J(\text{H,H}) = 2.5$ Hz, 1H each, H2), 6.16 and 6.11 (d, $J(\text{H,H}) = 2.5$ Hz, 2H each, H4 and H5), 1.31 and 1.30 (s, 18H each, Cp^{II}); ¹³C{¹H} NMR (75 MHz, CDCl₃, 25 °C): $\delta = 184.9$ (d, $J(\text{Rh-C}) = 74$ Hz, CO), 175.4 (CO), 149.4 and 149.1 (C1 and C3), 126.2 and 122.5 (C2), 110.1 and 110.0 (C4 and C5), 34.9 and 34.8 (CMe₃), 32.2 (CH₃, Cp^{II}); MS (FAB⁺, CH₂Cl₂): m/z (%): 916 (46) [M^+], 860 (100) [$M^+ - 2\text{CO}$], 739 (49) [$M^+ - \text{Cp}^{\text{II}}$]; IR (CH₂Cl₂): $\bar{\nu}(\text{CO}) = 2062$ (s), 2031 (s), 1996 (m), 1971 cm⁻¹ (m).

- [9] P. Kalck, C. Serra, C. Machet, R. Broussier, B. Gautheron, G. Delmas, G. Trouvé, M. Kubicki, *Organometallics* **1993**, *12*, 1021.
- [10] Crystal data for **3**: C₃₆H₅₄IrO₂RhS₂Zr, $M_r = 969.24$, monoclinic, space group $P2_1/c$; $a = 11.9123(9)$, $b = 21.5742(17)$, $c = 15.0796(12)$ Å, $\beta = 105.526(2)^\circ$, $V = 3734.0(5)$ Å³, $Z = 4$, $\rho_{\text{calcd}} = 1.724$ g cm⁻³, $\mu = 4.407$ mm⁻¹. Crystal dimensions 0.12 × 0.16 × 0.18 mm. Bruker SMART CCD diffractometer, $T = 153(1)$ K, graphite-monochromated MoK α radiation ($\lambda = 0.71073$). A complete hemisphere of data was scanned on ω (0.30° per frame) with a run time of 20 s at the detector resolution of 512 × 512 pixel. Reflections were extracted by using the SAINT program, and Lorentzian, polarization, and absorption corrections were applied. Of 9398 reflections measured, 4506 were unique ($R_{\text{int}} = 0.0657$). The structure was solved by direct methods (SHELXS-97) and refined by full-matrix least squares on F^2 (SHELXL-97). Anisotropic displacement parameters were used for all non-hydrogen atoms. Hydrogen atoms were included in calculated positions. 403 parameters, 18 restraints; $R = 0.0509$ (3512 reflections, $F \leq 4\sigma(F_o)$), $R_w(F^2) = 0.1007$ (all reflections), and $S = 1.076$. Max. residual electron density 1.05 e Å⁻³ close to the Ir atom. Crystallographic data (excluding structure factors) for the structure reported in this paper have been deposited with the Cambridge Crystallographic Data Centre as supplementary publication no. CCDC-116623. Copies of the data can be obtained free of charge on application to CCDC, 12 Union Road, Cambridge CB21EZ, UK (fax: (+44)1223-336-033; e-mail: deposit@ccdc.cam.ac.uk).
- [11] A. A. Del Paggio, E. L. Muettterties, D. M. Heinekey, V. W. Day, C. S. Day, *Organometallics* **1986**, *5*, 575.
- [12] F. H. Antwi-Nsiah, O. Oke, M. Cowie, *Organometallics* **1996**, *15*, 1042.
- [13] R. McDonald, M. Cowie, *Inorg. Chem.* **1990**, *29*, 1564.
- [14] Z. Tang, Y. Nomura, Y. Ishii, Y. Mizobe, M. Hidai, *Organometallics* **1997**, *16*, 151.
- [15] a) I. F. Urazowski, V. I. Ponomaryov, O. G. Ellert, I. E. Nifant'ev, D. A. Lemenovskii, *J. Organomet. Chem.* **1988**, *356*, 181; b) W. A. King, S. Di Bella, A. Gulino, G. Lanza, I. L. Fragalà, C. L. Stern, T. Marks, *J. Am. Chem. Soc.* **1999**, *121*, 355.
- [16] C. H. Winter, D. A. Dobbs, X.-X. Zhou, *J. Organomet. Chem.* **1991**, *403*, 145.
- [17] a) J. Okuda, *J. Organomet. Chem.* **1988**, *35b*, C43; b) C. H. Winter, X.-X. Zhou, M. J. Heeg, *Inorg. Chem.* **1992**, *31*, 1808.

Photomodulation of the Conformation of Cyclic Peptides with Azobenzene Moieties in the Peptide Backbone**

Raymond Behrendt, Christian Renner, Michaela Schenk, Fengqi Wang, Josef Wachtveitl, Dieter Oesterhelt, and Luis Moroder*

For photomodulation of conformational, physico-chemical, and biological properties of peptides, proteins, and phospholipids large use has been made of the *cis/trans* isomerization of azobenzene moieties grafted to specific sites of such biomaterials or related model systems.^[1, 2] Since the light-induced isomerization of azobenzene is accompanied by significant changes in geometry and polarity of the chromophore,^[3] this proved to be well suited for induction of local topochemical changes in conformationally more restricted small systems.^[4–10] Low-mass cyclic peptides are rigid structures that are extensively exploited for the design of libraries of conformers of defined bioactivities.^[11, 12] Thus, incorporation of the azobenzene moiety into the peptide backbone of such cyclic peptides is expected to represent an ideal system to probe the efficiency of this “light-switch” for induction of conformational transitions. With 4-(4-aminophenylazo)benzoyl (APB) as amino acid residue in the peptide backbone we succeeded in the present study to construct a very rigid, conformationally constrained cyclic peptide in the *trans* configuration which upon irradiation, relaxes into a largely free conformational space.

The distance between the two *para*-carbon atoms of the azobenzene unit in the *trans* configuration is 9 Å and in the *cis* configuration 5 Å. To transfer optimally these changes in geometry to the peptide backbone, H-APB-OH was synthesized according to known methods^[13] and fully characterized in its photochemical properties.^[14, 15] It was then incorporated into an octapeptide related to the active site of thioredoxine reductase (Scheme 1). Owing to the low nucleophilicity of the *para*-amino group of H-APB-OH, its protection in acylating the resin-bound peptide was not required, but difficulties were encountered in the subsequent acylation of this group. These were overcome by silylation and using the acid fluoride method for the peptide-chain extension step. Mild acidic cleavage from the resin produced the linear side chain protected pseudo-nonapeptide **1**, which was then cyclized by the PyBOP/HOBt/DIEA procedure. Final acidic deprotection generated the target compound **2** cyclo(Ala-Cys(SiBu)-Ala-Thr-Cys(SiBu)-Asp-Gly-Phe-APB).

Peptides **1** and **2** were characterized spectroscopically (Table 1). Compared to H-APB-OH [$\lambda_{\text{max}} = 420$ nm ($\pi - \pi^*$)

[*] Prof. Dr. L. Moroder, Dipl.-Chem. R. Behrendt, Dr. C. Renner, Dr. M. Schenk, Dr. F. Wang, Prof. Dr. D. Oesterhelt
Max-Planck-Institut für Biochemie
Am Klopferspitz 18A, D-82152 Martinsried (Germany)
Fax: (+49) 89-8578-2847
E-mail: moroder@biochem.mpg.de
Dr. J. Wachtveitl
Institut für Medizinische Optik der Universität
Oettingenstrasse 67, D-80538 München (Germany)

[**] The study was supported by the SFB 533 (grant A8 Moroder/Oesterhelt).

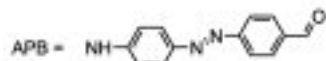


Table 1. Spectroscopic parameters of **1** and **2** in DMSO. The extinction coefficients ($\text{M}^{-1} \text{dm}^3 \text{cm}^{-1}$) were calculated from two isomeric mixtures; the different *cis/trans* isomer ratios were determined quantitatively from ^1H NMR spectra.

and 440 nm ($n-\pi^*$)^[14] the $\pi-\pi^*$ transition in both the linear and cyclic peptide is significantly blue-shifted, while the $n-\pi^*$ transition is located at similar wavelengths. The evolution of the *cis/trans* photoisomerization upon irradiation at 360 nm and 450 nm, respectively, shows for both the peptide **1** and **2** two isosbestic points at 330 and 440 nm which indicate that the photoreaction follows a first-order kinetic, as exemplified for **2** in Figure 1. A comparison of the thermal isomerization rates of the cyclic peptide **2** with those of the linear peptide **1** indicates an enhanced hindrance of the *cis* \rightarrow *trans* isomerization by the peptide backbone in the cyclized form

© WILEY-VCH Verlag GmbH, D-69451 Weinheim, 1999

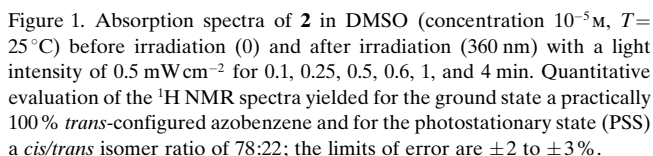


Table 2. Rate constants k_{ct} of the *cis* \rightarrow *trans* thermal isomerization of **1** and **2** in DMSO determined by ^1H NMR spectroscopy at different temperatures (peptide concentration $3 \times 10^{-3}\text{ M}$). The activation energy E_a was determined from Arrhenius plots; the limits of error are $\pm 10\text{ kJ mol}^{-1}$.

at 22 °C is markedly slower than that of the free azobenzene derivative H-APB-OH, in which this process is completed in about 10 min. Thus, the slow thermal relaxation of compound **2** ($t_{1/2}$ = 62 h at 22 °C) allowed ^1H NMR experiments to be performed for the conformational analysis of the *cis* isomer.

obtain a photoswitchable two-state system with a transition from a rigid to a flexible peptide conformation. Therefore this bis(cysteinyI)-peptide was selected for our model studies to eventually allow for further conformational restriction through disulfide bridging to the bicyclic form, if required. As shown in Figure 2, already the monocyclic peptide with *trans*-configured azobenzene moiety is fully constrained in its conformational space. The azobenzene moiety is planar and the peptide backbone displays an overall extended rigid structure; only residue 5 exhibits dihedral angles of the α -helical type. While in the *trans* isomer primarily a 180° flip-flop of the azobenzene moiety is observed, in the *cis* isomer the free rotation of the two phenyl rings is restricted by mutual hindrance and by steric effects of the peptide moiety.

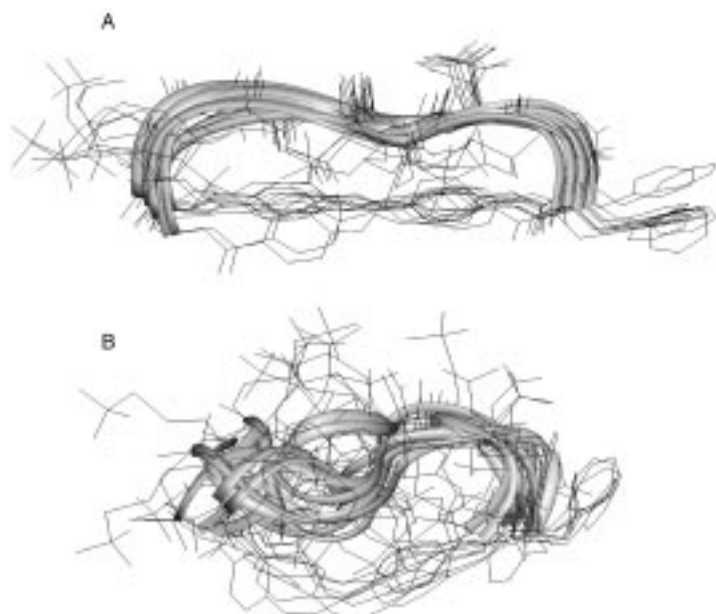


Figure 2. Ensembles of the ten structures of lowest energy for cyclo(Ala-Cys(SrBu)-Ala-Thr-Cys(SrBu)-Asp-Gly-Phe-APB) (**2**) in the *trans* (A) and *cis* configuration (B).

Even the peptide backbone is relaxed in the *cis* isomer into a significantly less constrained conformational space (Figure 2B). In its C-terminal peptide sequence a γ -turn centered on Gly-7 is largely populated, which fluctuates in an unconcerted mode with the rest of the peptide. The remaining part of the peptide chain bulges into a loose turnlike structure with a strongly 3_{10} -helical residue in position 4 and less helical Ala-3 and Cys-5 residues, which reflects the intrinsic tendency of this peptide portion to form an ordered fold. This makes the *cis* isomer a frustrated system consisting of an ensemble of energetically degenerate states. The N-terminus of the peptide part finally forms a short turn to the azobenzene moiety.

By using 4-(4-(aminomethyl)phenylazo)benzoic acid as building block in the cyclic octapeptide, as previously proposed by Ulysse et al.,^[9] the *cis* \rightleftharpoons *trans* photoisomerization leads again to a conformational transition which, however, is less pronounced. In fact, under identical conditions the peptide moiety, already in the *trans*-configured azobenzene, exhibits two different conformations in a ratio of 3:1, as determined by NMR conformational analysis. Conversely, by using the chromophore APB that lacks the flexible methylene spacer we obtained a peptide template, whose photoisomerization proceeds in a two-state transition. It therefore represents a promising system for spectroscopic analysis of this conformational transition on different time scales, also because of the high quantum yields ($\Phi_{ic} \approx 20\%$ and $\Phi_{ci} \approx 50\%$ for the $n\text{-}\pi^*$ transition).^[18] Correspondingly, this template should also allow photomodulation of biological properties of peptidic receptor ligands.

Experimental Section

1: The linear peptide was synthesized by applying Fmoc/tBu chemistry on chlorotrityl resin (PepChem, Tübingen) and was cleaved from this with CH_2Cl_2 /trifluoroethanol/AcOH/triethylsilane. HPLC (Nucleosil 300/C18 (Machery & Nagel, Düren), linear gradient of acetonitrile/2 % H_3PO_4 from

5/95 to 80/20 in 30 min): $t_r = 28$ min; FAB-MS: m/z : 1320 $[M+\text{Na}^+]$; $M_r = 1297.4$ calcd for $\text{C}_{60}\text{H}_{57}\text{N}_{11}\text{O}_{13}\text{S}_4$; amino acid analysis (6 M HCl; 110°C ; 24 h): Asp 1.00 (1) Thr 0.75 (1) Gly 1.00 (1) Ala 1.94 (2) Cys 1.64 (2) Phe 0.94 (1); peptide content: 95 %

2: The linear peptide **1** was cyclized with PyBOP/HOBt/DIEA in DMF and the resulting compound was deprotected with trifluoroacetic acid/ CH_2Cl_2 /triethylsilane (95/3.5/1.5). The crude product was precipitated with diethyl ether and purified by extensive washings with MeOH; HPLC (Nucleosil 300/C18 (Machery & Nagel, Düren), linear gradient of acetonitrile/2 % H_3PO_4 from 5/95 to 80/20 in 30 min): $t_r = 24.35$ min; ESI-MS: m/z : 1168.4 $[M+\text{H}^+]$; $M_r = 1167.2$ calcd for $\text{C}_{52}\text{H}_{69}\text{N}_{11}\text{O}_{13}\text{S}_4$; amino acid analysis (6 M HCl; 110°C ; 24 h): Asp 1.01 (1) Thr 0.85 (1) Gly 1.00 (1) Ala 1.96 (2) Cys 1.65 (2) Phe 0.99 (1); peptide content: 93 %.

UV spectra were recorded at a peptide concentration of 10^{-5} M in DMSO on a Lambda 19 spectrometer (Perkin Elmer). A xenon lamp 450 XBO (Osram, München) was used for irradiation at 360 nm (filter from Itos, Mainz) with a light intensity of 0.5 mW cm^{-2} .

The ^1H NMR experiments (500.13 MHz, 295 K) were recorded on a Bruker AMX 500 spectrometer equipped with pulsed-field-gradient (PFG) accessories. The signals were assigned according to the method of Wüthrich.^[19] The 2D TOCSY spectra were recorded with a spin-lock period of 70 ms using the MLEV-17 sequence for isotropic mixing.^[20] Experimental distance constraints (*trans*-azo: 44; *cis*-azo: 41) were extracted from 2D NOESY experiments^[21] with mixing times of 50 ms and 200 ms and from 2D ROESY experiments with a mixing time of 100 ms. Angle constraints (*trans*-azo: 18; *cis*-azo: 12) were extracted from 2D DQF-COSY^[22] and simple ^1H -1D spectra. Structure calculations and evaluations were performed with the INSIGHTII (version 97.0) software package from MSI by simulating the solvent DMSO with a dielectric constant of 46.7. Structures were first generated by a distance geometry algorithm and subsequently refined with a short simulated annealing molecular dynamics protocol. The experimental constraints were applied at every stage of the calculation. To check for the stability of the resulting structures, molecular dynamics simulations over a period of 1 ns were performed for representative members of the structure ensembles. No significant violations of experimental constraints occurred for any of the calculated structures.

Received: February 25, 1999 [Z13081IE]
German version: *Angew. Chem.* **1999**, *111*, 2941–2943

Keywords: azo compounds • conformation analysis • isomerizations • peptides • solid-phase synthesis

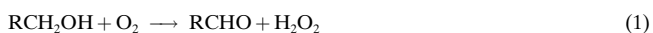
- [1] I. Willner, S. Rubin, *Angew. Chem.* **1996**, *108*, 419–439; *Angew. Chem. Int. Ed. Engl.* **1996**, *35*, 367–385.
- [2] I. Willner, *Acc. Chem. Res.* **1997**, *30*, 347–356.
- [3] H. Rau in *Studies in Organic Chemistry: Photochromism, Molecules and Systems*, Vol. 40 (Eds.: H. Dürr, H. Bonas-Laurent), Elsevier, Amsterdam, **1990**, pp. 165–192.
- [4] H.-W. Losensky, H. Spelthann, A. Ehlen, F. Vögtle, J. Bargon, *Angew. Chem.* **1988**, *100*, 1225–1227; *Angew. Chem. Int. Ed. Engl.* **1988**, *27*, 1189–1191.
- [5] K. H. Neumann, F. Vögtle, *J. Chem. Soc. Chem. Commun.* **1988**, 520–522.
- [6] M. S. Voller, T. D. Clark, C. Steinem, M. Z. Ghadiri, *Angew. Chem.* **1999**, *111*, 1703–1706; *Angew. Chem. Int. Ed.* **1999**, *38*, 1598–1606.
- [7] T. Aoyagi, A. Ueno, M. Fukushima, T. Osa, *Macromol. Rapid Commun.* **1998**, *19*, 103–105.
- [8] T. Nagasaki, S. Tamagaki, K. Ogino, *Chem. Lett.* **1997**, 717–718.
- [9] L. Ulysse, J. Cubillos, J. Chmielewski, *J. Am. Chem. Soc.* **1995**, *117*, 8466–8467.
- [10] S. Rudolph-Böhner, M. Krüger, D. Oesterhelt, L. Moroder, T. Nägele, J. Wachtveitl, *J. Photochem. Photobiol. A* **1997**, *105*, 235–248.
- [11] G. Müller, M. Gurrath, H. Kessler, *J. Comput. Aided Mol. Des.* **1994**, *8*, 709–730.
- [12] H. R. Haubner, D. Finsinger, H. Kessler, *Angew. Chem.* **1997**, *109*, 1440–1456; *Angew. Chem. Int. Ed. Engl.* **1997**, *36*, 1375–1389.

- [13] K. H. Schündehütte in *Houben-Weyl, Methoden Org. Chem. (Houben-Weyl) 4th ed. 1965–, Vol. 10/3*, p. 240.
- [14] J. Wachtveitl, T. Nägele, B. Puell, W. Zinth, M. Krüger, S. Rudolph-Böhner, D. Oesterhelt, L. Moroder, *J. Photochem. Photobiol. A* **1997**, *105*, 283–288.
- [15] T. Nägele, R. Hoche, W. Zinth, J. Wachtveitl, *Chem. Phys. Lett.* **1997**, *272*, 489–495.
- [16] L. Moroder, D. Besse, H.-J. Musiol, S. Rudolph-Böhner, F. Siedler, *Biopolym. Pept. Sci.* **1996**, *40*, 207–234.
- [17] J. Kuriyan, T. S. R. Krishna, L. Wong, B. Guenther, A. Pahler, C. H. Williams, Jr., P. Moldel, *Nature* **1991**, *352*, 172–174.
- [18] J. Wachtveitl, T. Nägele, A. J. Wurzer, M. Schenk, L. Moroder in *Springer Series in Chemical Physics, Vol. 63* (Eds.: T. Elsaesser, J. G. Fujimoto, D. A. Wiersma, W. Zinth), Springer, Stuttgart, **1998**, pp. 609–611.
- [19] K. Wüthrich, *NMR of Proteins and Nucleic Acids*, Wiley, New York, **1986**.
- [20] A. Bax, D. G. Davis, *J. Magn. Reson.* **1985**, *65*, 355–360.
- [21] J. Jeener, B. H. Meier, P. Bachman, R. R. Ernst, *J. Chem. Phys.* **1979**, *71*, 4546–4553.
- [22] M. Rance, O. W. Sorensen, G. Bodenhausen, G. Wagner, R. R. Ernst, K. Wüthrich, *Biochem. Biophys. Res. Commun.* **1983**, *117*, 479–485.

Oxidation of Benzyl Alcohol with Cu^{II} and Zn^{II} Complexes of the Phenoxyl Radical as a Model of the Reaction of Galactose Oxidase**

Shinobu Itoh,* Masayasu Taki, Shigehisa Takayama, Shigenori Nagatomo, Teizo Kitagawa, Norio Sakurada, Ryuichi Arakawa, and Shunichi Fukuzumi*

Redox interactions between a transition metal ion and a redox-active amino acid side chain such as the phenol group of tyrosine have been recognized to play a crucial role in several biologically important processes.^[1] Recently, a tyrosyl radical directly coordinated to a Cu^{II} center has been discovered in the active site of galactose oxidase (GO, EC 1.1.3.9), which catalyzes the oxidation of D-galactose and primary alcohols to the corresponding aldehydes, coupled to the reduction of O₂ to H₂O₂ [Eq. (1)].^[1, 2] The crystal structure of GO at 1.7-Å resolution clearly shows that the tyrosine



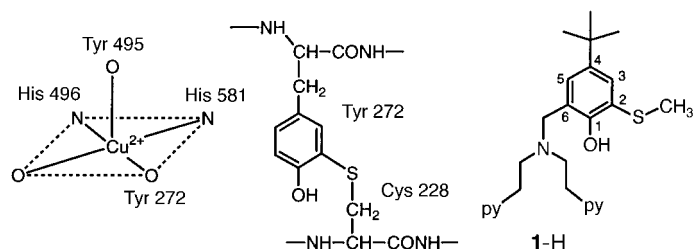
[*] Dr. S. Itoh, Prof. S. Fukuzumi, M. Taki, S. Takayama
Department of Material and Life Science
Graduate School of Engineering, Osaka University
2-1 Yamada-oka, Suita, Osaka 565-0871 (Japan)
Fax: (+81) 6-6879-7370
E-mail: fukuzumi@chem.eng.osaka-u.ac.jp

Dr. S. Nagatomo, Prof. T. Kitagawa
Institute for Molecular Science
Myodaiji, Okazaki 444-8585 (Japan)

N. Sakurada, Prof. R. Arakawa
Department of Applied Chemistry
Faculty of Engineering, Kansai University
3-3-35 Yamate-cho, Suita, Osaka 564-8680 (Japan)

[**] This study was financially supported in part by a Grant-in-Aid for Scientific Research on Priority Area (Molecular Biometallics: 10129218; Electrochemistry of Ordered Interface: 10131242) and a Grant-in-Aid for General Scientific Research (08458177) from the Ministry of Education, Science, Culture, and Sports of Japan.

residue (Tyr272), which is directly coordinated to a Cu²⁺ ion at the equatorial position, is covalently bound to the sulfur atom of the adjacent Cys228, constituting a new organic cofactor (Scheme 1).^[2] The active form of GO has recently been suggested to be the Cu^{II}–phenoxyl radical of this organic cofactor, which is converted into the two-electron reduced species [Cu^I(phenol)] in the oxidation of alcohols to aldehydes.^[3–6]



Scheme 1. Representation of the coordination at the Cu^{II} center of galactose oxidase (left; the unlabeled O atom is from an acetate ion or water), the organic cofactor (center), and the protonated form of the ligand used in the model complexes **1** (right; py = 2-pyridyl).

Extensive efforts have been made recently to develop synthetic model complexes that can mimic the catalytic function and the spectroscopic characteristics of the Cu^{II}–phenoxyl radical species of the native enzymes.^[7–10] Wieghardt et al. have succeeded in developing a very unique functional model of GO using 2,2'-thiobis(4,6-di-tert-butylphenol) (LH₂) as the ligand; this complex can oxidize alcohols under aerobic conditions.^[7b] In this system the active species has been shown to be the dimeric phenoxyl radical complex [Cu^{II}(L[•])₂]²⁺, in which only the radicals act as oxidation sites and no redox reaction occurs at the Cu^{II} site. Now the important question remains as to the essential role of the Cu^{II} site.

We report herein two synthetic model complexes whose structures and spectroscopic features are similar to those of the active form of GO. One is a Cu^{II}–phenoxyl radical complex that can accept two electrons, and the other is a Zn^{II}–phenoxyl radical complex that can accept only one electron. To our surprise, both model complexes can oxidize benzyl alcohol to yield the same product, benzaldehyde. The important difference between the two model complexes is found to lie in the different kinetic formulation for the oxidation of the alcohol. These features of our model complexes provide valuable insights into the catalytic mechanism of GO.

Addition of (NH₄)₂[Ce^{IV}(NO₃)₆] (ceric ammonium nitrate, CAN) to a solution of the dimeric copper(II)–phenolate complex [Cu^{II}(**1**)₂](PF₆)₂ (2.5 × 10^{−4} M in CH₃CN)^[11] caused an immediate decrease in the absorption band at 522 nm due to the dimeric copper(II)–phenolate complex (ligand-to-metal charge-transfer (LMCT) transition from the phenolate to the Cu²⁺ ion), accompanied by the concomitant increase in the new absorption bands at 415 nm (ε = 1790 M^{−1} cm^{−1}) and 867 nm (ε = 550 M^{−1} cm^{−1}) at 25 °C (Figure 1). A similar spectrum was obtained in the oxidation of [Zn^{II}(**1**)-(CH₃CN)]PF₆^[11] by CAN under the same experimental conditions (418 nm (ε = 1250 M^{−1} cm^{−1}) and 887 nm (ε = 510 M^{−1} cm^{−1}) in CH₃CN at 25 °C). The absorption bands in